# Hyperfine structure and homogeneous broadening in $Pr^{3+}:KY(WO_4)_2$

H. L. Xu, M. Nilsson, S. Ohser, N. Rauhut, and S. Kröll
*Department of Physics, Lund Institute of Technology, P.O. Box 118, S-22100 Lund, Sweden*

M. Aguiló and F. Díaz
*Laboratori de Fisica Aplicada i Cristallografia, Universitat Rovira i Virgili, 43007 Tarragona, Spain*
(Received 30 June 2004; published 30 December 2004)

As part of a search for suitable materials for coherent quantum operations, relaxation times and hyperfine structure of the $^1D_2(1)$-$^3H_4(1)$ transition in $Pr^{3+}:KY(WO_4)_2$ (0.29 at. %) at 4 K have been obtained using photon-echo and spectral hole burning techniques. The homogeneous linewidth and the effect of excitation-induced dephasing were measured using two-pulse photon-echo techniques. Linewidths of $23.4\pm1.0$ and $17.6\pm0.9$ kHz were obtained in the absence and presence of an external magnetic field of about 9 mT. The radiative lifetime ($T_1$) of the $^1D_2$ state was measured to be $43\pm2$ $\mu$s using time-resolved laser-induced fluorescence and three-pulse photon-echo measurements. The transmission hole spectra were measured and directly yielded the quadrupole level splitting in the $^1D_2$ ($3.77\pm0.03$ and $4.58\pm0.04$ MHz) and $^3H_4$ ($17.1\pm0.1$ and $33.2\pm0.3$ MHz) states. The spectral hole lifetime due to population redistribution between the ground-state nuclear levels was also determined to be $70\pm10$ ms. A strong dipole-dipole interaction observed in this crystal opens for potential applications in quantum computing schemes for performing quantum logic operations, but the short dephasing time makes it less useful in data storage applications.

DOI: 10.1103/PhysRevB.70.214115 PACS number(s): 42.50.Md, 42.62.Fi, 78.55.−m

## I. INTRODUCTION

Rare-earth-ion-doped crystals are used in experiments within the areas of optical data storage and processing,[1–6] quantum information and computing,[7–9] as well as for frequency standards.[10,11] The spectroscopic properties of the materials determine their usefulness for the various applications and it is of interest to expand the range of available materials and to search for materials with properties even more suited for particular applications. Properties that make these materials attractive include the exceptionally narrow homogeneous optical linewidths,[12,13] or equivalently, the long dephasing time, and the ability to create (semi-) persistent spectral holes through optical pumping to metastable levels. The large ratio between the homogeneous and the inhomogeneous linewidths in these materials provide the basis for frequency and time domain data storage and the narrow spectral holes have provided frequency references for laser stabilization to less than 1 kHz at a range of optical wavelengths.[11]

Recently rare-earth-ion-doped materials have been used in quantum optical experiments, such as the demonstration of slow light based on the method of electromagnetically induced transparency[14] and in experiments aimed at using the dopant ions as quantum computer hardware.[8,15,16] In both cases, the spin transitions and the properties of the hyperfine levels are highly relevant. In the quantum computing scheme in Ref. 8 the long-lived hyperfine states are used as qubit states and spectral hole burning is used to prepare an ensemble of ions in a specific state, absorbing at a specific frequency within the inhomogeneously broadened absorption profile.

The quantum computing schemes exploit another property of rare-earth ions in solids, namely ion-ion coupling through electrostatic dipole interaction. In a crystal host, the ions can have a permanent electric dipole moment, which changes when an ion is optically excited. This in turn changes the resonance frequency of nearby ions, through dipole-dipole interaction, which leads to a line-broadening mechanism known as excitation induced frequency shifts.[17] For many applications, this effect is detrimental, since it increases the effective homogeneous linewidth, but in quantum computing schemes it can be used in a controlled manner to perform quantum logic operations. The investigation presented here was motivated by the search for new materials with long optical coherence times and strong ion-ion interaction for use in few qubit quantum computing applications.

$Pr:KY(WO_4)_2$ was identified as a material that could possess the useful properties mentioned above and was subjected to further studies. Praseodymium is an attractive ion since it has only one naturally occurring isotope, which makes spectral analysis simpler, and because Pr ions often have higher transition strengths and stronger electrostatic dipole coupling than, e.g., $Eu^{3+}$ ions in similar hosts. Many $Pr^{3+}$-doped materials have been investigated, in particular $Pr^{3+}:Y_2SiO_5$,[18,19] which has been used for experiments concerning quantum optics and quantum computing.[14] The constituents of the host material $KY(WO_4)_2$ have relatively low nuclear magnetic moments, which is favorable since homogeneous broadening is often caused by spin fluctuations where the magnetic moments of the host lattice nuclei couple to the dopant ions.[20] The main contribution in this host comes from $^{39}K$, with an isotope abundance of 93% and a nuclear magnetic moment of $0.39\mu_N$.

In this paper, we report the hyperfine structure and the homogeneous broadening in a $Pr^{3+}$ doped $KY(WO_4)_2$ crystal with a $Pr^{3+}$ concentration of 0.29% using photon-echo and hole-burning techniques. The paper is organized as follows. Section II describes basic material properties and the experi-

 

mental apparatus. The experimental results are given in Sec. III, in which the homogeneous linewidth, hyperfine structures, and spectral hole lifetimes are discussed in detail in Secs. III A, III B, and III C, respectively. Finally some conclusions are drawn in Sec. IV.

## II. EXPERIMENT

$Pr^{3+}:KY(WO_4)_2(KY_{0.9971}Pr_{0.0029}(WO_4)_2)$ single crystals have been grown by the top seeded solution growth (TSSG) method using a $K_2W_2O_7$ solvant. Crystal growth experiments were carried out at 948–925 K at the 31.41 $K_2O$:1.90 $Y_2O_3$:0.02 $Pr_2O_3$:66.67 $WO_3$ point of the phase diagram (molar ratio). Details of the growth procedure have been explained previously.[21]

The Pr concentration in the sample has been determined to be 0.29% by electron probe microanalysis, using CAMECA Camebax SX50 equipment. The crystal host, $KY(WO_4)_2$, belongs to the monoclinic system, space group $C2/c$, with unit parameters $a=1.06313(4)$, $b=1.03452(6)$, $c=0.75547(3)$nm, $\beta=130.752(2)$, and $Z=4$.[22] The $Pr^{3+}$ ions substituting for $Y^{3+}$ ions are coordinated with eight oxygen atoms, which form a distorted tetragonal antiprism (Thompson cube) having $C_2$ site symmetry.

The measurements were made on the lowest crystal-field states of the zero-phonon $^3H_4$-$^1D_2$ transition in $Pr^{3+}:KY(WO_4)_2$ at 613.07 nm. The sample was 5 mm long in the direction of light propagation and had a width and height of 3 and 5 mm, respectively, with three polished faces. The crystal was immersed in liquid helium and kept at a temperature of about 4 K. A Coherent CR-699-21 ring dye laser, pumped by a Spectra Physics 2080 argon–ion laser, operating with Rhodamine 6G provided a beam of light resonant with the optical transition $^3H_4$-$^1D_2$. The cw dye laser was linearly polarized and was operated in a single servo-locked mode with a nominal spectral width of ~1 MHz. The wavelength was determined by a Burleigh wavemeter (WA-4500).

In the photon-echo experiment and lifetime measurement, the light was gated by two Isomet 1205C acousto-optic modulators (AOMs), controlled by an Isomet D320 driver, creating excitation pulses with a duration in the interval 400–1200 ns at a repetition rate of 10 Hz. The two modulators were arranged such that the frequency of the light could be varied by changing the AOM rf carrier frequencies without changing the direction of the light. The light pulses were then focused on the crystal by a 20 cm focal-length lens to a beam diameter of ~0.15 mm. The light propagated along the *b* axis and the polarization was parallel to the *c* axis. In the photon-echo experiment, a third Isomet 1205 C acousto-optic modulator was put in the beam after the cryostat as a gate in order to block the excitation light and only allow the echo signal to pass through. The energy of the excitation pulses was measured by a Coherent Fieldmaster LM-2 power meter. The echo signal was detected by a photomultiplier tube (Hamamatsu R943-02) and recorded by a Tektronix 2431L oscilloscope. A static magnetic field of about 9 mT, provided by a pair of Helmholtz coils and oriented along the *b* axis, was also applied to the crystal in order to study how this affected the homogeneous linewidth. In the lifetime measurement, following pulsed excitation, a 40 cm focal-length lens was used to collect the fluorescence at right angles to the incident laser beam in order to avoid the influence of the optical free induction decay. The captured fluorescence was then focused on the photomultiplier tube and transferred to a Tektronix TDS 540 oscilloscope.

In the hole burning experiment, the spectral hole was probed by measuring the transmission of the laser with the intensity reduced by 2 – 3 orders of magnitude relative to the burning intensity. The two Isomet 1205C modulators used above were exchanged for an A&A Opto-Electronics acousto-optic modulator driven by a Tektronix AWG520 arbitrary wave form generator in order to obtain a wider frequency scanning range (200 MHz). The laser output was split into two beams. One was used to irradiate the crystal and the other was used as reference signal in order to eliminate the influence of fluctuations in laser amplitude. A matched pair of electronically amplified photodiodes (Hamamatsu S1223) was used for detection. The transmission hole spectrum and reference signal were recorded by the Tektronix TDS 540 oscilloscope and transferred to a computer, where the analyses of the spectra were performed.

## III. RESULTS AND DISCUSSION

### A. Homogeneous linewidth

The homogeneous linewidth of the $^1D_2$-$^3H_4$ transition was determined in time domain measurements using two-pulse photon echoes. The photon-echo signals decay, as a function of separation $\tau$ between the pulses, as $\exp(-4\tau/T_2)$, where $T_2$ is related to the homogeneous linewidth $\Gamma_h$ by $\Gamma_h=1/(\pi T_2)$. Typical parameters for the two excitation pulses in this experiment were pulse durations between 500 and 1200 ns and excitation intensities between 2.5 and 35 $W/cm^2$. The laser was continuously scanned over 1 GHz at a very slow rate (about 150 MHz/s) in order to avoid hole-burning effects during the photon echo experiments, while still ensuring spectral overlap of the two pulses within each excitation pulse pair. The pulse sequences were computer controlled and the echo intensities averaged over 30 echoes were recorded. The optical dephasing time was measured at several points in the absorption line, which had a maximum of absorption of about 80% (the absorption coefficient $\alpha$ is about 3.2 $cm^{-1}$). The resulting echo decay, with about 6 $W/cm^2$ excitation intensities, was 3.3 μs. This gives an optical dephasing time $T_2=13.2$ $\mu$s, yielding a homogeneous linewidth of $\Gamma_h=24.1$ kHz (see Fig. 1).

The homogeneous linewidth $\Gamma_h$ in $Pr^{3+}:KY(WO_4)_2$ arises from several dominant mechanisms, namely

$$\Gamma_h = \Gamma_0 + \Gamma_{\text{Pr-Pr}} + \Gamma_{\text{Pr-}Host} + \Gamma_{Phonon}, \tag{1}$$

where $\Gamma_0$ is the broadening due to the natural lifetime of the $^1D_2$ state, $\Gamma_{\text{Pr-Pr}}$ is due to $Pr^{3+}$-$Pr^{3+}$ interaction, and $\Gamma_{\text{Pr-}Host}$ is due to the $Pr^{3+}$-host interaction. The last term $\Gamma_{Phonon}$ describes the contribution due to coupling to phonons and consists of one-phonon direct processes, two-phonon Raman processes, two-phonon Orbach processes, and two-phonon

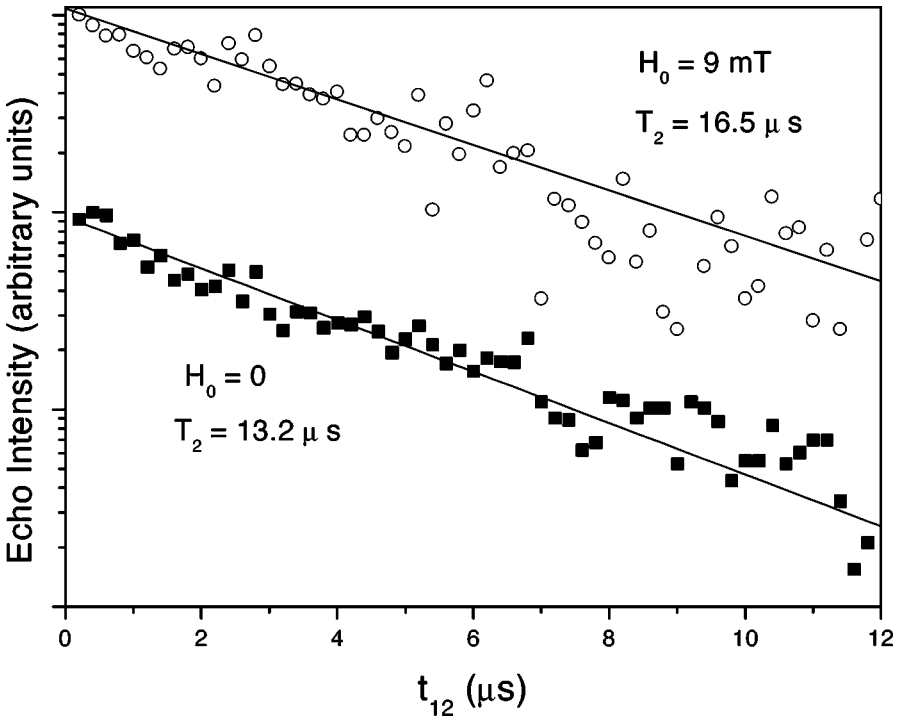


FIG. 1. Two-pulse photon echo decays on the $^1D_2$-$^3H_4$ transition in 0.29% $Pr^{3+}$:$KY(WO_4)_2$ at 4 K without a magnetic field ($H_0=0$) and with a magnetic field ($H_0=9$ mT) parallel to the *b* axis. The excitation intensity is about 6 W/cm$^2$ and the straight lines are exponential fits to the decays.

intrinsic Raman processes. Phonon broadening dominates at temperatures above a few Kelvin, but is strongly suppressed at 4 K.[23] In the present work, this temperature dependence of the homogeneous linewidth has not been studied. The $\Gamma_{\text{Pr-}Host}$ term comes from the guest-host interaction among the nuclear spins due to fluctuation of the local fields. This contribution depends strongly on the host crystal. The interaction is magnetic in origin and can be reduced to some extent by decoupling the host nuclei from the $Pr^{3+}$. Therefore, in this work, echo decays were also recorded in a static magnetic field of 9 mT to study the contribution to the linewidth from nuclear spin fluctuations of the host crystal. A reduction in homogeneous width was also observed as illustrated in Fig. 1. The echo decay with about 6 W/cm$^2$ excitation intensity gives a dephasing time $T_2=16.5$ $\mu$s, corresponding to a homogeneous linewidth of $\Gamma_h=19.3$ kHz. The application of the 9 mT magnetic field reduced the linewidth by about 5 kHz, showing the contribution from the host ions to the zero-field homogeneous linewidth and a relatively strong dependence of homogeneous linewidth on the magnetic properties of the host lattice.

The second term in Eq. (1), $\Gamma_{\text{Pr-Pr}}$, describes the contribution due to the excitation induced dephasing (instantaneous spectral diffusion) which is ascribed to the local multipole field or crystal field changes induced by the excitation of neighboring $Pr^{3+}$ ions.[12,17] Excitation of ions during the echo sequence shifts the transition frequencies of neighboring $Pr^{3+}$ ions because of the difference in electric dipole moments between the ground and the excited states, giving rise to a perturbation of phase relationships between the ions and a reduction of the echo intensity.[24] Therefore, the $\Gamma_{\text{Pr-Pr}}$ term strongly depends on the concentration of doped ions and the excitation intensity of the laser. In a crystal with a fixed concentration, the contribution of $\Gamma_{\text{Pr-Pr}}$ to the homogeneous linewidth $\Gamma_h$ can be extracted by plotting $\Gamma_h$ as a function of excitation energy, since the magnitude of the $\Gamma_{\text{Pr-Pr}}$ term is proportional to the density of excited $Pr^{3+}$ ions and is therefore directly proportional to the excitation density if the excitation density is weak enough that the pulse area is much smaller than $\pi$.[25] This can be explicitly expressed as

$$\Gamma_{\text{Pr-Pr}} = S_{\text{ISD}}\rho_e \tag{2}$$

where $\rho_e$ is the density of excited Pr ions and $S_{\text{ISD}}$ is the instantaneous diffusion slope. The excitation pulses in this experiment were attenuated by inserting neutral-density filters. Using the effective beam area ($A=\pi w_0^2/2$, where $w_0$ is the Gaussian beam waist), the excitation intensity and excitation density can be obtained. The homogeneous linewidth as a function of excitation intensity and excitation density is illustrated in Fig. 2. The broadening introduced by the measurement process itself is clearly seen and the decays extrapolated to zero excitation energy yielded a homogeneous linewidth of 23.4 kHz at zero field. For the 9 mT field case, extrapolation to zero excitation energy yields a homogeneous linewidth of 17.6 kHz. From Fig. 2, the instantaneous diffusion slope $S_{\text{ISD}}$ was found to be $3.5\times10^{-11}$ Hz cm$^3$. Due to the difficulty of determining the absolute laser intensity, the value will have a large uncertainty. Compared with the value found in other materials, e.g., $\sim1.4\times10^{-11}$ Hz cm$^3$ in $Pr^{3+}$:$Y_2SiO_5$,[18] and $\sim1\times10^{-12}$ Hz cm$^3$ in $Eu^{3+}$:$Y_2SiO_5$,[23] it is clear that there is a strong ion-ion interaction in this material, leading to a large $\Gamma_{\text{Pr-Pr}}$. The interaction is attributed to electric dipole interaction, which is proportional to $(\Delta\overline{\mu})^2$, where $\Delta\overline{\mu}$ is the difference between the static dipole moments of the ground and excited states. The exact value of $\Delta\overline{\mu}$ can be determined using Stark shift measurements.[26] A strong ion-ion interaction is important for the scheme for quantum computing in rare-earth-ion-doped crystals.[8,15,16]

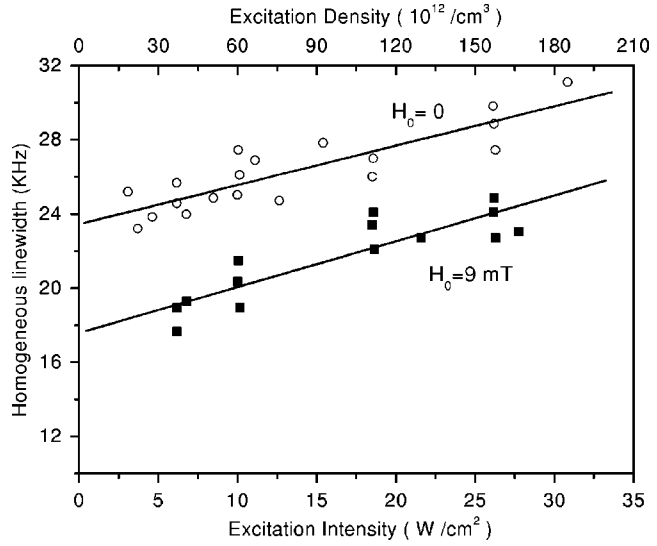


FIG. 2. Dependence of the homogeneous linewidths of the $^1D_2$-$^3H_4$ transition on the density of excited ions in the presence and absence of an external magnetic field.

The first term $\Gamma_0$ in Eq. (1) denotes the contribution arising due to the lifetime $T_1$ of the excited state $^1D_2$. $T_1$ was measured both by three-pulse photon echoes and by time-resolved laser-induced fluorescence. In the three-pulse photon echo experiment, the echo decay shows a decay time of 21 μs, resulting in a lifetime of $T_1$=42 $\mu$s. In order to avoid the possible contribution from long-lived hyperfine state storage to the echo intensity, the $^1D_2$ fluorescence lifetime was also measured by directly exciting the $^3H_4$-$^1D_2$ transition with a gated cw laser pulse of 1 μs duration and observing the exponential fluorescence decay. Since there is a large energy gap (>6000 $cm^{-1}$) between the $^1D_2$ state and the nearest lower energy state $^1G_4$ and the experiment was undertaken at low temperature, nonradiative decay may be neglected and the relaxation is dominated by radiative transitions from the $^1D_2$ state to the different lower states. The lifetime (43 μs) was thus obtained by monitoring the fluorescence from the $^1D_2$ state to all lower levels. The fluorescence decay curve is shown in Fig. 3, in which the inset illustrates the data obtained in the three-pulse photon echo experiment. A good agreement for the $^1D_2$ lifetime was found between these two methods. The lifetime of 43 μs contributes 3.7 kHz to the homogeneous linewidth. From the results obtained above, it can be observed that the extrapolated value to zero laser power in a 9 mT field is much larger than the ultimate limit of the homogeneous linewidth of 3.7 kHz, and therefore we conclude that there is still some residual contribution, for example from the interaction between the Pr ions and the host ions or possibly from the last term $\Gamma_{Phonon}$ due to coupling between the electronic levels and thermally excited phonons.

As a summary, Table I lists the parameters obtained in this crystal, as well as those obtained in $Pr^{3+}$-doped $Y_2SiO_5$ and $YAlO_3$.[18,27] In comparison with these other crystals $Pr^{3+}$:$KY(WO_4)_2$ has wider homogeneous and inhomogeneous linewidths, and a stronger interaction between dopant ions.

### B. Hyperfine structure

The hyperfine structures of the $^1D_2$ excited state and the $^3H_4$ ground state were directly determined in the frequency domain by spectral hole burning, in which transmission hole spectra were recorded. Due to the inhomogeneous broadening all allowed transitions between the hyperfine levels of the ground and excited states are resonant with the frequency of the burning laser for some subset of ions and a pattern of side holes and anti-holes can be recorded. The side holes are due to transitions from the ground state levels with depleted population to all of the excited state hyperfine levels and the antiholes are due to population redistribution between the ground state hyperfine levels, giving rise to enhanced absorp-

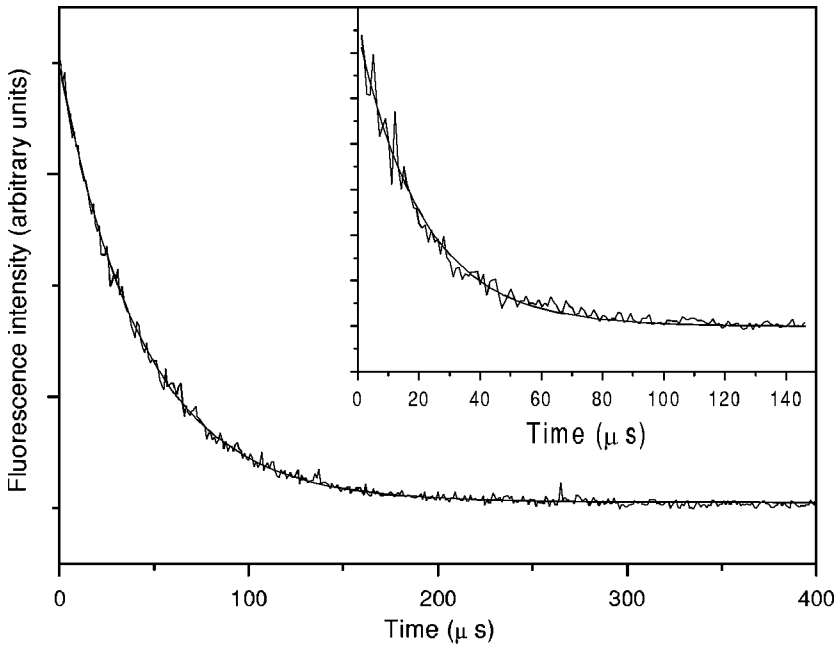


FIG. 3. Time-resolved fluorescence from the $^1D_2$-$^3H_4$ transition. The exponential fit gives a lifetime ($T_1$) of 43 μs. The inset shows a three-pulse photon echo decay with an exponential fit that yielded a decay ($T_1/2$) of 21 μs.

TABLE I. Spectral and relaxation parameters for the $^1D_2(1)$-$^3H_4(1)$ transition in 0.29% $Pr^{3+}:KY(WO_2)_4$, together with comparable data for $Pr^{3+}:YAlO_3$ and $Pr^{3+}:Y_2SiO_5$.

| Crystal | $Pr^{3+}:KY(WO_4)_2$ (0.29%) | $Pr^{3+}:YAlO_3$ (0.1%)[a] | $Pr^{3+}:Y_2SiO_5$ (0.02%)[b] Site 1 | Site 2 |
|---|---|---|---|---|
| $\lambda$ | 613.07 nm | 610.5 nm | 605.977 nm | 607.934 nm |
| $\Gamma_{hom}$ | 23.4±1.0 kHz ($H_0$=0) | 4.5 kHz ($H_0$=0) | 2.4 kHz ($H_0$=0) | 1.05 kHz ($H_0$=0) |
| $\Gamma_{hom}$ | 17.6±0.9 kHz ($H_0$=90 G) | 2.0 kHz ($H_0$=80 G) | 1.8 kHz ($H_0$=77 G) | 0.85 kHz ($H_0$=77 G) |
| $\Gamma_{inhom}$ | >25 GHz | 5 GHz | 4.4 GHz | 2.5 GHz |
| $T_1$ | 43±2 $\mu$s | 160 μs | 164 μs | 222 μs |
| $T_{HF}$ | 70±10 ms | — | >100 s[c] | >100 s[c] |
| $S_{ISD}$ | $3.5\times10^{-11}$ Hz cm$^3$ | — | $1.2\times10^{-11}$ Hz cm$^3$ | $1.4\times10^{-11}$ Hz cm$^3$ |

[a]See Ref. 27.
[b]See Ref. 18.
[c]See Ref. 19.

tion features. This can be used to determine the hyperfine splitting of the two states. The Pr nucleus has a spin of $I=5/2$, and the nuclear quadrupole interaction and the second-order hyperfine coupling split the $^1D_2$ excited state and the $^3H_4$ ground state into three hyperfine levels ($I_z=\pm1/2,\pm3/2,\pm5/2$). In this case, a pattern of three sideholes and 21 antiholes are expected on each side of the burning laser frequency (primary hole). The frequency intervals between the primary hole and sideholes give the hyperfine level splittings of the excited state, whereas the frequency intervals between the primary hole and antiholes yield the hyperfine level splittings of the ground state, as well as the sum and difference of the splittings in the excited state and the ground state.

In this experiment, the burning pulse duration was changed from 0.5 to 20 ms and the burning intensity was 2—3 orders of magnitude larger than the intensity of the readout pulse. The readout pulse was scanned over a range from 20 to 200 MHz in the spectral vicinity of the burning pulse and had a duration between 20 and 800 μs. In Fig. 4, a typical transmission spectrum of holes and antiholes is presented. The overall hole picture of the ground and excited states was obtained by irradiating for 5 ms and probing by letting the laser scan once over 150 MHz during 800 μs. The separation between the burning and reading pulses is 1 ms and recording is done in a single shot in order to avoid laser-frequency jitter which will decrease the resolution of the hole spectrum. In Fig. 5, the transmission hole spectra for the $^1D_2$-$^3H_4$ transition with a higher frequency resolution is shown. The probe pulse was scanned over 20 MHz during 200 μs. A resonant hole width of about 0.5 MHz, limited by laser-frequency jitter and readout chirp rate, was achieved. As shown in Fig. 5, the resolution is sufficient for determining the splitting in the $^1D_2$ excited state.

The frequencies of the excited-state and the ground-state splittings and the results are summarized in Table II. The values were compared with numerical simulation of the hole-burning spectra from the observed hyperfine splittings as illustrated by solid lines in Figs. 4 and 5. The theoretical analysis was performed using a simple linear-absorption

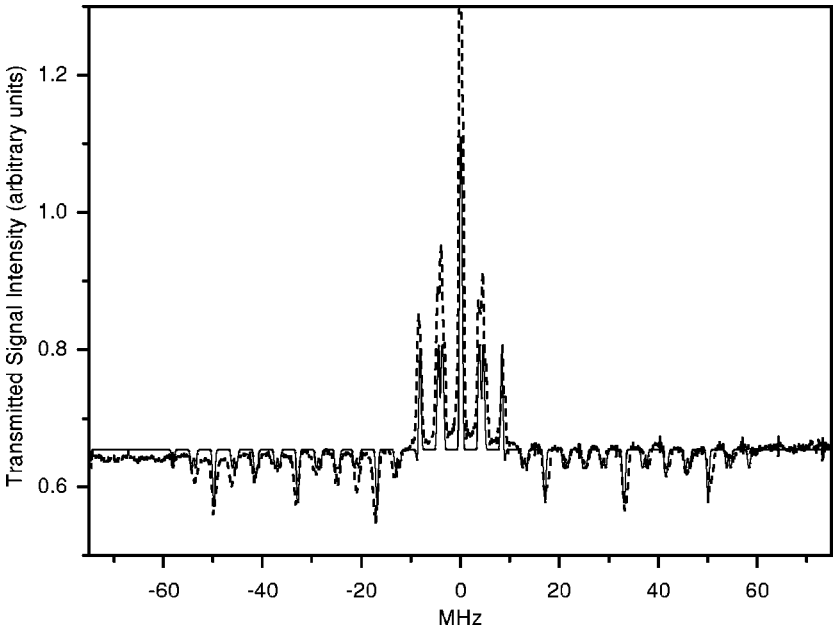


FIG. 4. Experimentally obtained (dashed line) and theoretically fitted (solid line) transmission hole spectra for the transition between the lowest crystal-field split components of the $^1D_2$ and $^3H_4$ states.

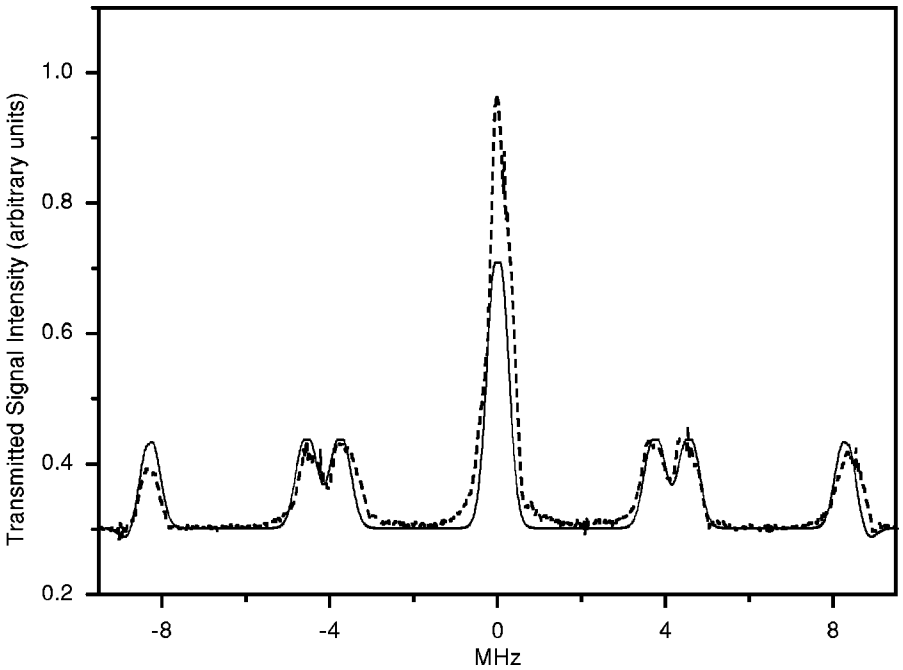


FIG. 5. Experimentally obtained (dashed line) and theoretically fitted (solid line) transmission hole spectra for the $^1D_2$-$^3H_4$ transition in a higher frequency resolution for determination of the hyperfine splittings of the $^1D_2$ state.

model. The burned primary hole, sideholes, and antiholes were assumed to be Gaussian in shape and to have a 0.5 MHz width at half maximum. The transition probabilities for all possible pairs of the hyperfine levels between the ground state and the excited state were assumed to be the same. It was also assumed that the relaxation only takes place from the $^1D_2$ state to the ground state and the population is equally distributed among the remaining two hyperfine levels. As can be seen in Figs. 4 and 5, there is good consistency between the experimental and simulated spectra. The measured hyperfine splittings can be used for calculating the combined quadrupole and second-order-hyperfine coupling constants $D$ and $E$ in the effective quadrupole Hamiltonian $H_Q = D[I_z^2 - I(I+1)/3] + E(I_x^2 - I_y^2)$.[20] In our experiment, the ordering of the hyperfine splittings of the $^1D_2$ excited state and the $^3H_4$ ground state was not determined. Therefore, the signs of $D$ and $E$ cannot be specified. The hyperfine coupling constants $D$ and $E$ were fitted according to the procedures as presented in Ref. 28 and they are also listed in Table II.

### C. Spectral hole lifetime

In this work, the lifetime of the spectral holes was also measured by burning a hole in the absorption line and subsequently probing the spectral hole after a variable time. The spectral hole lifetime depends on the rate of population redistribution among the ground-state hyperfine levels, which can be due to several possible mechanisms including direct one-phonon process, two-step Orbach processes, inelastic Raman scattering, and spectral diffusion through $Pr^{3+}$-$Pr^{3+}$ interaction.[23] The hole was measured by scanning the laser frequency with intensity attenuated by a factor of $10^3$–$10^4$ in comparison with the burning pulse in order to avoid that the probing laser affected the hole decay. The spectral hole depth as a function of the time separation between the burning and probing laser pulses is illustrated in Fig. 6. A single exponential fit gives a lifetime ($T_{HF}$) of 70 ms. The estimated single exponential value is the effective overall lifetime for the hole relaxation process, since different spin-lattice relaxation rates among the three hyperfine levels is possible. The contribution to spectral hole lifetime due to direct one-phonon processes (absorption and emission of phonons) can be very slow because the phonon density at the hyperfine splitting frequency is very low. However, the contribution of the remaining three mechanisms to the hyperfine level relation could not be distinguished, since our experiments did not explore the dependence of hole refilling on temperature and concentration.

TABLE II. The splitting between hyperfine levels of the $^3H_4$ and $^1D_2$ states together with the hyperfine coupling constants $D$ and $E$. Our experiments did not determine the ordering of the hyperfine levels and the signs of the constants are not specified.

| Frequency (MHz) | Ground state $^3H_4$ | Excited state $^1D_2$ |
|---|---|---|
| $\delta_1$ | 17.1 | 3.77 |
| $\delta_2$ | 33.2 | 4.58 |
| $\delta_1+\delta_2$ | 50.3 | 8.35 |
| $\lvert D\rvert$ | 8.34 | 1.25 |
| $\lvert E\rvert$ | 0.419 | 0.321 |

## IV. CONCLUSION

In summary, the techniques of photon echo and spectral hole-burning have been applied to $Pr^{3+}$-doped $KY(WO_4)_2$. The dephasing mechanisms and spectroscopic properties of $Pr^{3+}$ ions in this crystal were investigated. The homogeneous linewidth of the optical transition from the $^3H_4(1)$ ground state to the $^1D_2(1)$ excited state was determined and the contributions to the linewidth were also identified by studying the effects of excitation-intensity-dependent dephasing and the influence of a magnetic field. A strong dipole-dipole in-

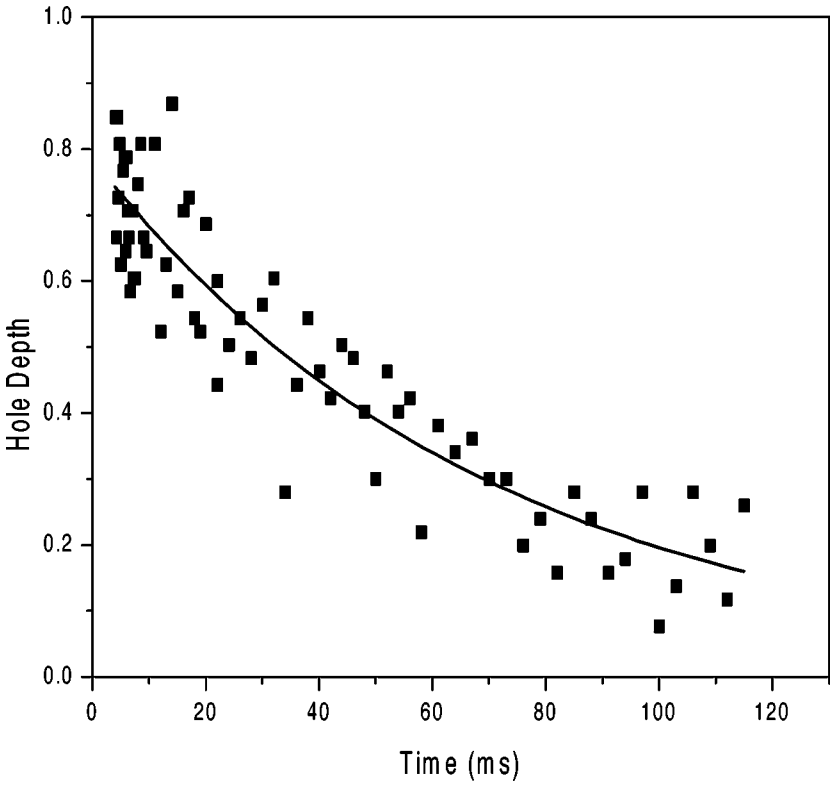


FIG. 6. The time decay of holes burnt in 0.29% $Pr^{3+}:KY(WO_2)_4$. The detected hole intensity (squares) and an exponential fit (solid line), which gives a lifetime of 70 ms.

teraction in this material was observed, which can be helpful in quantum computing schemes for performing quantum logic operations. On the other hand, the homogeneous dephasing time is considerably shorter than in $Pr^{3+}:Y_2SiO_5$, which is a disadvantage for several applications. Using the spectral hole-burning technique, the quadrupole level splittings of the $^1D_2$ and $^3H_4$ states in this crystal were resolved and accurately assigned. The hyperfine coupling constants $D$ and $E$ were also obtained. The results reported are relevant to those searching for new materials for various potential practical applications with regard to optical amplifiers, phosphors, laser stabilization, laser emission, and optical data processing.

## ACKNOWLEDGMENTS

The authors would like to thank Professor Moncorgé at the University of Caen for selecting an appropriate crystal material and acknowledge support from the ESQUIRE project within the IST-FET program of the EU, the Swedish Research Council, and the Knut and Alice Wallenberg Foundation.

[1] H. Lin, T. Wang, and T. W. Mossberg, Opt. Lett. **20**, 1658 (1995).
[2] X. A. Shen, D. An-Dien, J. W. Perry, D. L. Huestis, and R. Kachru, Science **278**, 96 (1997).
[3] W. R. Babbitt and J. A. Bell, Appl. Opt. **33**, 1538 (1994).
[4] T. L. Harris, Y. Sun, W. R. Babbitt, R. L. Cone, J. A. Ritcey, and R. W. Equall, Opt. Lett. **25**, 85 (2000).
[5] E. S. Maniloff, A. E. Johnson, and T. W. Mossberg, MRS Bull. **24**, 46 (1999)
[6] I. Lorgere, L. Menager, V. Lavielle, J.-L. Le Gouet, D. Dolfi, S. Tonda, and J.-P. Huignard, J. Mod. Opt. **49**, 2459 (2002).
[7] M. D. Lukin, and P. R. Hemmer, Phys. Rev. Lett. **84**, 2818 (2000).
[8] M. Nilsson, L. Rippe, N. Ohlsson, T. Christiansson, and S. Kröll, Phys. Scr., T **102**, 178 (2002).
[9] J. J. Longdell, and M. J. Sellars, Phys. Rev. A **69**, 032307 (2004).
[10] G. J. Pryde, T. Bottger, R. L. Cone, and R. C.C. Ward, J. Lumin. **98**, 309 (2002)
[11] P. B. Sellin, N. M. Strickland, T. Bottger, J. L. Carlsten, and R. L. Cone, Phys. Rev. B **63**, 155111 (2001).
[12] R. W. Equall, Y. Sun, R. L. Cone, and R. M. Macfarlane, Phys. Rev. Lett. **72**, 2179 (1994)
[13] Y. Sun, C. W. Thiel, R. L. Cone, R. W. Equall, and R. L. Hutcheson, J. Lumin. **98**, 281 (2002)
[14] A. V. Turukhin, V. S. Sudarshanam, M. S. Shahriar, J. A. Musser, B. S. Ham, and P. R. Hemmer, Phys. Rev. Lett. **88**, 023602 (2002).
[15] N. Ohlsson, R. K. Mohan, and S. Kröll, Opt. Commun. **201**, 71 (2002).
[16] J. J. Longdell, M. J. Sellars, and N. B. Manson, Phys. Rev. Lett. **93**, 130503 (2004).
[17] J. Huang, J. M. Zhang, A. Lezama, and T. W. Mossberg, Phys. Rev. Lett. **63**, 78 (1989)
[18] R. W. Equall, R. L. Cone, and R. M. Macfarlane, Phys. Rev. B **52**, 3963 (1995).

[19] K. Holliday, M. Croci, E. Vauthey, and U. P. Wild, Phys. Rev. B **47**, 14 741 (1993).
[20] R. M. Macfarlane, and R. M. Shelby, in *Spectroscopy of Solids Containing Rare Earth Ions*, edited by A. A. Kaplyanskii and R. M. Macfarlane (North-Holland, Amsterdam, 1987), Chap. 3.
[21] M. C. Pujol, C. Zaldo, R. Solé, V. Nikolov, X. Solans, M. Aguiló, and F. Díaz, Appl. Phys. B: Lasers Opt. **68**, 187 (1999).
[22] M. C. Pujol, X. Mateos, R. Solé, Jna. Gavaldà, J. Massons, M. Aguiló, and F. Díaz, Mater. Sci. Forum **378-381**, 710 (2001); S. V. Borisov and R. F. Kletsova, Sov. Phys. Crystallogr. **13**, 420 (1968).
[23] F. Könz, Y. Sun, C. W. Thiel, R. L. Cone, R. W. Equall, R. L. Hutcheson, and R. M. Macfarlane, Phys. Rev. B **68**, 085109 (2003).
[24] S. Kröll, E. Y. Xu, and R. Kachru, Phys. Rev. B **44**, 30 (1991).
[25] R. Yano, M. Mitsunaga, and N. Uesugi, J. Opt. Soc. Am. B **9**, 992 (1992).
[26] F. R. Graf, A. Renn, U. P. Wild, and M. Mitsunaga, Phys. Rev. B **55**, 11 225 (1997).
[27] R. M. Macfarlane, R. M. Shelby, and R. L. Shoemaker, Phys. Rev. Lett. **43**, 1726 (1979).
[28] A. Wokaun, S. C. Rand, R. G. DeVoe, and R. G. Brewer, Phys. Rev. B **23**, 5733 (1981).